# DFIG-based wind turbine advanced control strategy employing a combination of PSO and artificial neural networks.

K.S.Ramanjaneyulu[1], S.Yogendravarma[2], V.Sai[3], L.Sambamurthy[4], S.Sivaramkrishna[5], and A.Sateesh[6].

[1] *Associate Professor, Dept of EEE, NSRIT, Vishakapatnam, AP*

[2,3,4,5,6] *B.tech Students, Dept of EEE, NSRIT, Vishakapatnam, AP*

*NSRIT-Nadimpalli Satyanarayana Raju Institute of Technology*

**Abstract—An enhanced control approach for wind turbines based on DFIG is proposed in this research. The proposed approach is predicated on a hybrid of Artificial Neural Network (ANN) and Particle Swarm Optimisation (PSO). To track the available maximum power point (MPPT) at different wind speeds, PSO combined ANN is recommended. PSO is therefore employed to optimise the Proportional Integral (PI) controller gains of the Doubly Fed Induction Generator (DFIG), so improving its dynamic performance. The performance of the PSO-optimized PI controller in comparison to the conventional one is highlighted in this paper. Via a 2 MW DFIG-WT, the suggested control technique is validated using the MATLAB/Simulink environment. The acquired findings confirm that the suggested PSO-PI is a useful technique for enhancing DFIG WT's dynamic behaviour. It shows that, in comparison to the traditional PI, the overshoots are 50% lower. Additionally, the suggested control method produces a quicker transient reaction.**

**Keywords: Particle Swarm Optimisation (PSO), Artificial Neural Network (ANN), Double Fed Induction Generator (DFIG), Wind Turbine, MPPT.**

## I. INTRODUCTION

Although fossil fuels remain the primary energy source for the world's economy, their recognition as a primary contributor to environmental issues compels people to look for alternate energy sources [1], [2]. Furthermore, a growing interest in renewable energies has been fostered by the declining reserves of fossil fuels and the rising usage of electrical energy[3], [4]. With its major benefits, such plenty and cleanliness, wind energy is a viable and crucial way to meet the world's expanding need for electricity. In recent years, it has gained more attention. Despite being plentiful, wind energy fluctuates constantly as wind speed changes. As a result, maximum power point tracking, or MPPT, is essential to wind energy conversion systems in order to minimise the installation's return on investment while simultaneously maximising system efficiency. Numerous wind energy conversion system topologies are proposed by the extensive research documented in the literature. The most popular of these is the grid-connected DFIG that is linked to a wind turbine with variable speed (WT). Due to its many benefits, including independent control over both active and reactive power, cheap converter costs, and less mechanical stress, this system has been widely implemented in the wind industry [1], [4].

The rotor windings of a DFIG are linked to the grid via a series of back-to-back converters, which are made up of the grid-side converter (GSC) and the rotor-side converter (RSC). A DFIG is simply an induction generator with a wound rotor. Only 20% to 30% of the nominal generator's power may be transferred by the converters in this setup [1], [4], [5].

Using PI controllers, control of the decoupled currents of both converters allows for control of the back-to-back converters. The primary disadvantage of this kind of control, though, is that it heavily depends on the proper configuration of the PI parameters for the DFIG-based generating system's operation [6]. An oscillatory dynamic behaviour and even system instability might result from improperly configuring the controller's settings [5].

This work provides an enhanced meta-heuristics based on PSO to enhance the dynamic performance of PI controllers. In order to reach global optima, this algorithm has a high convergence rate and the right amount of variety. The PSO gain setting of PI controllers utilised in the control loops of the DFIG-based wind turbine is expanded in this article. To create a sensorless MPPT controller that tracks the maximum power point in the face of changing environmental circumstances, the same algorithm is linked to an artificial neural network.

This is how the rest of the paper is organised. Section II discusses the theoretical concept and control of DFIG-based WT. The suggested MPPT control approach utilising ANN coupled PSO and the best way to tune PI controllers using PSO are explained in Section III. The performance of the suggested control technique is shown in Section IV, and the conclusion is presented in Section V.

## II. DFIG BASED WECS MODEL AND CONTROL

A. Wind Turbine Model The wind turbine output power is expressed as follows [7]:

$$P_{Turbine} = \frac{1}{2}\rho A C_p(\lambda,\beta)V_\omega^3 \tag{1}$$

where A is the area that the turbine blades sweep (in meters squared), is the air density (in kilogrammes per m3), and Cp is the power conversion coefficient, which may be written as follows:

$$\lambda = \frac{\omega_m R}{V_\omega} \tag{2}$$

where m and R stand for the turbine blades' formed radius (in m) and the shaft's angular speed (in rad s), respectively. Additionally, the power conversion coefficient Cp is an onlinear function of the tip-speed ratio, which has a specific maximum opt, and the turbine pitch angle (in degrees). The maximum power thus has the following expression:

$$P_{Turbine_{Max}} = \frac{1}{2}\rho A C_{pMax} V_\omega^3 \tag{3}$$

The wind turbine's mechanical torque is expressed as follows:

$$T_m = \frac{1}{2\omega_m}\rho A C_p(\lambda,\beta)V_\omega^3 \tag{4}$$

The power conversion coefficient Cp(), which describes the wind turbine, is modelled using a generalised equation and is written as follows:

$$C_p(\lambda,\beta) = \frac{1}{2}\left(\frac{116}{\lambda_i} - 0.4\beta - 5\right)e^{\left(-\frac{21}{\lambda_i}\right)} \tag{5}$$

$$\frac{1}{\lambda_i} = \frac{1}{\lambda + 0.08\beta} - \frac{0.035}{\beta^3+1} \tag{6}$$

Figure 1 depicts the Cp( ) form at various pitch angles. For = 0o and Opt=81, the highest value of the power conversion coefficient CpMax = 0411 is achieved.As a result, regardless of changes in wind speed, the tip-speed ratio needs to be kept at its ideal value in order to maximise the extracted power. As a result, there is an ideal rotating speed for agivenwind speed that preserves TSR equality at the ideal ratio.Because of this, it is feasible to calculate the maximum power that a wind turbine PTurbineMax can produce by utilising an MPPT system, which controls the turbine's rotational speed to a number that keeps the TSR at optimal.

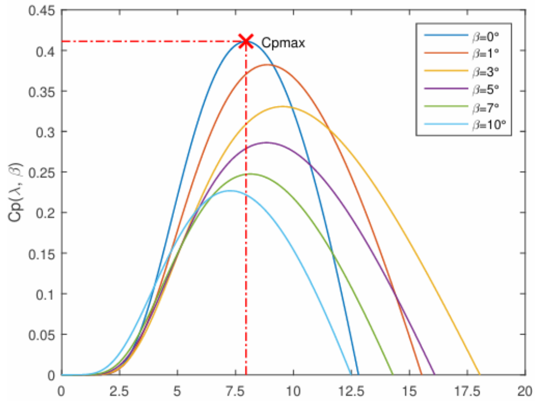


Fig.1. Characteristic of the power conversion coefficient Cp( )at different pitch angles .

The dynamice quation of the WECS is given as follows[8]:

$$J\frac{d\omega_m}{dt} = T_e - T_m - F\omega_m \tag{7}$$

where J is the system's moment of inertia, F is the viscous friction coefficient, Tm is the mechanical torque produced by the turbine, and Te is the electromagnetic torque produced by the turbine-driven generator.

B. Modelling of the DFIG The dynamic equations of the DFIG are expressed as follows[9], [10]:

$$\begin{cases} v_{ds} = R_s i_{ds} + \dfrac{d\phi_{ds}}{dt} - \phi_{qs}\omega_s \\ v_{qs} = R_s i_{qs} + \dfrac{d\phi_{qs}}{dt} + \phi_{ds}\omega_s \end{cases} \tag{8}$$

$$\begin{cases} v_{dr} = R_r i_{dr} + \dfrac{d\phi_{dr}}{dt} - \phi_{qr}\omega_r \\ v_{qr} = R_r i_{qr} + \dfrac{d\phi_{qr}}{dt} + \phi_{dr}\omega_r \end{cases} \tag{9}$$

The stator and rotor flux linkages are given by[9], [10]:

$$\begin{cases} \phi_{ds} = L_s i_{ds} + L_m i_{dr} \\ \phi_{qs} = L_s i_{qs} + L_m i_{qr} \end{cases} \quad (10)$$

$$\begin{cases} \phi_{dr} = L_r i_{dr} + L_m i_{ds} \\ \phi_{qs} = L_r i_{qr} + L_m i_{qs} \end{cases} \quad (11)$$

The DFIG electromechanical torque is expressed as follows:

$$T_{em} = \frac{3pL_m}{2L_s}(\phi_{qs} i_{dr} - \phi_{ds} i_{qr})$$

C. Control of the DFIG based WECS

For DFIG-based WECS, vector control is the most often utilised technique. Under typical operating conditions, cascaded vector control systems, which are implemented in an asynchronous rotating Q-frame, are commonly utilised for power converter control [11].

Two cascaded control loops make up the RSC converter's control architecture. The purpose of the inner current loops is to independently regulate the rotor current component, which is used to manage the stator's reactive power, and the component iqr. The spinning speed of DFIG is regulated by the outside control loop.

The active and reactive powers of the stator side are given by the following expressions[10]:

$$\begin{cases} P_s = Re(\overline{V}_s * i_s^*) = \frac{3}{2}(v_{ds} i_{ds} + v_{qs} i_{qs}) \\ Q_s = Im(\overline{V}_s * i_s^*) = \frac{3}{2}(v_{qs} i_{ds} - v_{ds} i_{qs}) \end{cases} \quad (13)$$

As seen in Fig. 2, the vector control of the DFIG is carried out in an asynchronous rotating dq frame, where the axis d is aligned with the stator flux space vector.

$$\begin{cases} v_{ds} = \frac{d\phi_s}{dt} = 0 \\ v_{qs} = \phi_s \omega_s = v_s \end{cases} \quad (14)$$

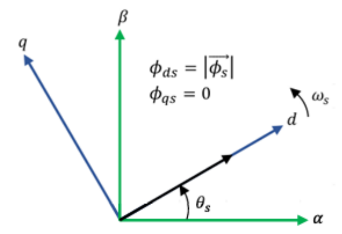


Fig.2. Synchronous rotating dq reference frame aligned with the stator flux space vector.

The $dq$ current components are given as follows:

$$\begin{cases} i_{ds} = \frac{v_{qs}}{\omega_s L_s} - \frac{L_m}{L_s} i_{dr} \\ i_{qs} = -\frac{L_m}{L_s} i_{qr} \end{cases} \quad (15)$$

Finally, the $dq$ fluxes are expressed by:

$$\begin{cases} \phi_{dr} = L_r \sigma i_{dr} + \frac{\omega_s L_m}{L_s} v_{qs} \\ \phi_{qr} = L_r \sigma i_{qr} \end{cases} \quad (16)$$

where $\sigma = 1 - \frac{L_m^2}{L_s L_r}$ is the machine leakage coefficient.
The active and reactive stator powers expressions become:

$$\begin{cases} P_s = \frac{-3L_m}{2L_s} v_{qs} i_{qr} \\ Q_s = \frac{-3L_m}{2L_s} v_{qs} i_{dr} + \frac{3}{2\omega_s L_s} v_{qs}^2 \end{cases} \quad (17)$$

Equation (17) implies that there is a decoupling between the control of the statator's active and reactive capabilities. The component iqr controls the stator active power. The component IDR may regulate the active power if the grid sets the voltage and frequency.

In order to be able to manage the machine appropriately, it is vital to define the relationship between the currents and the rotor voltages that will be applied to the machine. the expressions inserted in (9) by equation (16) result in:

$$\begin{cases} v_{dr} = R_r i_{dr} + L_r \sigma \frac{di_{dr}}{dt} - L_r \sigma i_{qr} \omega_r \\ v_{qr} = R_r i_{qr} + L_r \sigma \frac{di_{qr}}{dt} + \omega_r (L_r \sigma i_{dr} + \frac{L_m}{\omega_s L_s}) \end{cases} \quad (18)$$

The gridside converter's purpose is to control the voltage and reactive power of the DC connection. Independent management of the DC link voltage and the reactive power flowing between the grid and the GSC is made possible by the use of vector control approaches with reference frames orientated along the grid voltage vector.

Here is how the grid's reactive and active powers are expressed:

$$\begin{cases} P_g = Re(\overline{V}_g * i_g^*) = \frac{3}{2}(v_{dg} i_{dg} + v_{qg} i_{qg}) \\ Q_g = Im(\overline{V}_g * i_g^*) = \frac{3}{2}(v_{qg} i_{dg} - v_{dg} i_{qg}) \end{cases} \quad (19)$$

By decomposing into dq components, the basic equations of the filter $(R_f, L_f)$ connected to the grid are given bellow [10]:

$$\begin{cases} v_{df} = R_f i_{dg} + L_f \dfrac{di_{dg}}{dt} + v_{dg} - L_f i_{qg}\omega_s \\ v_{qf} = R_f i_{qg} + L_f \dfrac{di_{qg}}{dt} + v_{qg} + L_f i_{dg}\omega_s \end{cases} \quad (20)$$

The $d$ axis of the rotating frame is aligned with the grid voltage space vector $\overrightarrow{V_g}$, The resulting $dq$ components of the grid voltage yield to:

$$\begin{cases} v_{dg} = \overrightarrow{V_g} \\ v_{qg} = 0 \end{cases} \quad (21)$$

Therefore, eq. (20) is simplified to:

$$\begin{cases} v_{df} = R_f i_{dg} + L_f \dfrac{di_{dg}}{dt} + v_{dg} - L_f i_{qg}\omega_s \\ v_{qf} = R_f i_{qg} + L_f \dfrac{di_{qg}}{dt} + L_f i_{dg}\omega_s \end{cases} \quad (22)$$

The active and reactive grid powers become:

$$\begin{cases} P_g = Re(\overline{V}_g * i_g^*) = \dfrac{3}{2} v_{dg} i_{dg} \\ Q_g = Im(\overline{V}_g * i_g^*) = -\dfrac{3}{2} v_{dg} i_{qg} \end{cases} \quad (23)$$

The overall proposed control scheme for DFIG based WT is shown in Fig. 3.

THEPROPOSEDCONTROLSTRATEGY

The gridside converter's purpose is to control the voltage and reactive power of the DC connection. Independent management of the DC link voltage and the reactive power flowing between the grid and the GSC is made possible by the use of vector control approaches with reference frames orientated along the grid voltage vector.

Here is how the grid's reactive and active powers are expressed:

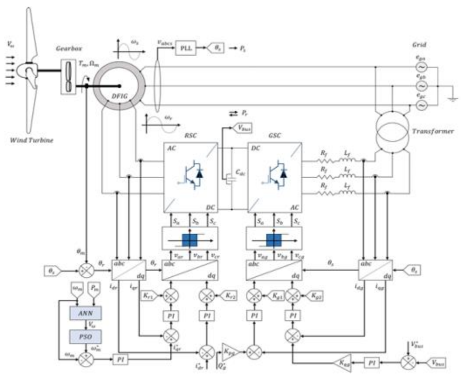


Fig. 3. Proposed DFIG control scheme.

It has one purelin neurone in the output layer, two linear neurones in the input layer, ten tan-sigmoid neurones in the first hidden layer, eight tan-sigmoid neurones in the second hidden layer, and five tan-sigmoid neurones in the third hidden layer. Next, the ANN's output is provided by:

$$y(k) = W_4 f^3(W_3 f^2(W_2 f^1(W_1 u(k) + b_1) + b_2) + b_3) \quad (24)$$

where u = [Pm m] is the neural network's input, y is its output, b1, b2, and b3 are the bias vectors, f1, f2, and f3 are the tan-sigmoid activation functions, and W1, W2, W3, and W4 are the weight matrices.

C. Particle Swarm Optimization (PSO)

Metaheuristics that draw inspiration from the social behaviour of swarming animals in the wild have been proposed recently. Particle Swarm Optimisation (PSO) in particular. Particles are a collection of random possible solutions that are the initial state of the process. These particles move in a multidimensional search space, modifying their locations in response to both their own and other particles' experiences, in an attempt to find the best solution [15], [16].

Based on the mechanical power curves presented in Figure 4 and prior discussions, the turbine power reaches its peak at a shaft rotational speed known as the optimum speed, or Opt. Therefore, for any wind speed, the wind turbine must rotate at this optimal speed in order to extract the greatest power. By altering the electromagnetic torque produced by the DFIG, the wind turbine's rotational speed may be adjusted.

PSO is a population of solutions based search technique. It generally generates Np particles in the search space at random [15]. Each particle j has a position in the search space of Xk j and a velocity of Vk j at time t. In the following iteration (Xk+1 j, Vk+1 j), each particle's position and velocity change [17]. The problem's solutions are represented by each location of the particle Xk j (in our example, the m rotational speed reference and [KpKi] PI gains), and the variation of each position around the Min and Max of the solution domain is represented by Vk j.

The optimal performance function at iteration k (the maximum of the objective function for maximisation problems and its minimum for minimisation problems; in our case, it is the rotational speed m maximising the objective function F1 and [KpKi] minimising the objective function F2) is stored in a memory that each particle possesses. This position is called Pbest. Gbest, which relates to the m and [KpKi] values evaluated by a population member and which provided the best performance in comparison with that of the entire population at iteration k, is the position where maximum performance has been recorded for every member in the population.

This idea takes into account a weighted random acceleration when switching from one iteration to the next [15]. Equation (25) provides a mathematical model for this situation. where the population size is represented by the formula j = 12 Np. is the inertia moment, which starts at 1 and gets smaller as the iteration goes on. A positive constant, rand, is a random integer between 0 and 1, and k is the number of iterations that actually occur. The typical motion mechanism of a particle in the search space is shown in Fig. 6.

Finding the rotational speed m that maximises the power function at any wind speed is the task for the MPPT. The following definition applies to the objective function that is maximised:

$$F_1 = Max\left[\frac{1}{2}\rho A C_p(\lambda, \beta) V_\omega^3\right] \tag{26}$$

Finding the settings [Kp Ki KpidrKqidrKpiqrKqiqr] that guarantee the least amount of overshoot and the fastest reaction time is the key to fine-tuning PI controller gains.

The DFIG control system's dynamic performance is assessed using the ITAE criterion. The following is the expression for the index ITAE [18], [19]:

$$F_2 = Min\left[\int_0^\infty t.((\omega_m^* - \omega_m) + (i_{dr}^* - i_{dr}) + (i_{qr}^* - i_{qr}))\mathrm{d}t\right] \tag{27}$$

Algorithm 1 describes the hole population's optimisation procedure.

## III. SIMULATION RESULTS AND ANALYSIS

To evaluate the effectiveness of the proposed control strategy, the simulation tests are performed under different wind conditions in the MATLAB/Simulink software. Tab. I

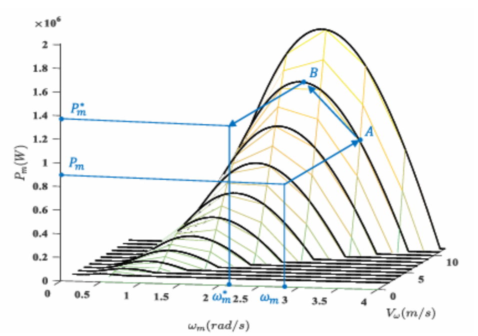


Fig. 4. Characteristic of the turbine power $P_m(V_\omega, \omega_m)$.

**Algorithm 1:** Pseudo-code of PSO algorithm.

**Result:** The algorithm return the optimal rotation speed $\omega_m^*$ and the optimal gains of PI controllers $[K_p^*, K_i^*]$ as $G_{best}$.
Random initialization of $N_p$ $[X_j(1, 2, ..., N_p)]$ population of particles, coefficients $c_1$, $c_2$, and $\omega$;
Calculate fitness function for each population member.
$P_{best}(X_j)$= Performance at the initial position of each particle.
$G_{best}$= Performance at the particle position with the best performance.
**while** $It < MaxIt$ **do**
  **for** $j = 1 : N_p$ **do**
    Update position and velocity of each particle according to eq. (25).
    Calculate the fitness function $f(X_j)$ for each member of the population.
    **if** $f(X_j) > P_{best_{X_j}}$ **then**
      $P_{best_{X_j}} = f(X_j)$; Personal best updating.
    **end**
    **if** $f(X_j) > G_{best}$ **then**
      $G_{best} = f(X_j)$; Global best updating.
    **end**
  **end**
  Decrease $\omega$,
  $It = It + 1$.
**end**

displays the findings that were achieved using the PSO MPPT. Tab. II provides a summary of the PSO algorithm's outcomes for PI tuning. Generator

In Tab. III, parameters are shown. In Tab. V, the PSO parameters are shown.

Fig. 7 displays the performance of the ANN. It is evident from this figure that the ANN provides reliable wind speed estimations. Figures 8, 9, and 10 show the results of the suggested optimisation strategy's performance under varying wind conditions. It is evident that when compared to the traditional PI controller, all of the performance metrics of the PSO-tuned PI are enhanced.

Furthermore, it is evident from Fig. 9 that the PSO-PI responds faster than the traditional PI; its rise time is estimated to be 022 s, compared to 025 s for the conventional PI. Additionally, overshoots recorded with PSO-tuned PI are much better; for the traditional controller, these parameters are assessed to 627% whereas the optimised controller only records an overshoot of 315 percent.

As a result, ITAE is 50% lower than with the traditional PI.

Based on the data obtained, it can be concluded that for the control of the DFIG based wind turbine, the PSO adjusted PI is more efficient than the traditional PI.

TABLE I

PSO MPPT SIMULATION RESULTS.

| Parameter | $V_\omega$=8 $m/s$ | $V_\omega$=10 $m/s$ |
|---|---|---|
| Maximum power $P_{Max}$ | 543716.4298 $W$ | 1069415.5069 $W$ |
| Optimal rotational speed $\omega^*_{mOpt}$ | 163.3 $rad/s$ | 204.62 $rad/s$ |

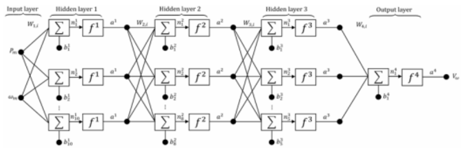


Fig.5. Proposed Multilayer ANN scheme for wind spee destimation. Fig(6)

$$\begin{cases} V_j^{(k+1)} = \omega V_j^{(k)} + c_1 rand[0,1]\left(P_{best} - X_j^{(k)}\right) + c_2 rand[0,1]\left(G_{best} - X_j^{(k)}\right) \\ X_j^{(k+1)} = X_j^{(k)} + V_j^{(k+1)} \end{cases} \quad (25)$$

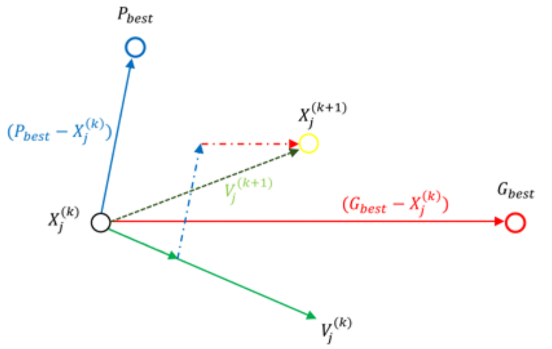


Fig.6. Typical displacement of a particle in the search space.

TABLEII

PIANDPSOTUNEDPIRESULTSSUMMARY.

| Parameter | $\omega_m$ PI | $i_{dr}$ PI | $i_{qr}$ PI |
|---|---|---|---|
| Conventional PI | | | |
| Proportional gain $K_p$ | 1000 | 0.5771 | 0.5771 |
| Integral gain $K_i$ | 5000 | 491.5995 | 491.5995 |
| PSO tuned PI | | | |
| Proportional gain $K_p$ | 1993.4 | 0.2737 | 0.4975 |
| Integral gain $K_i$ | 19898.7 | 617.9441 | 1359.7329 |

## IV. CONCLUSION

This research presents the establishment of an enhanced control method for DFIG-based wind turbines utilising a combined Artificial Neural Network and PSO Algorithm. Consequently, the suggested algorithm is used to extract the most wind power that is accessible. Furthermore, by fine-tuning PI settings that minimise the ITAE, high accuracy and quick reaction times are attained. The designed methodology has replaced the conventional approaches that rely on analytical calculations and are difficult to implement successfully with acceptable outcomes. Therefore, it can be said that the suggested approach performs very well for adjusting the PI controller settings of the DFIG-based wind system.

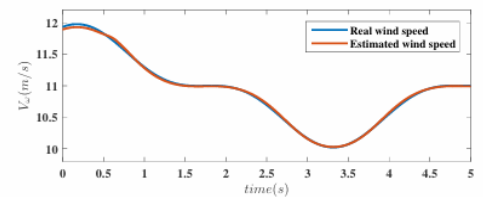


Fig. 7. ANN wind speed estimation results.

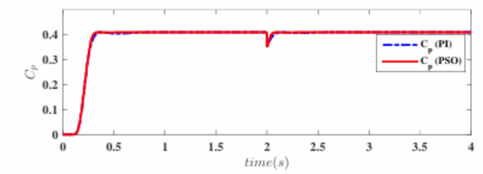


Fig. 8. Optimized $C_p$ response for MPPT control.

TABLEIII

WINDTURBINEPARAMETERS.

| Parameter | Value |
|---|---|
| $\rho$ Air density | 1.08 $kg/m^3$ |
| $A$ Area swept by turbine blades | 4775.94 $m^2$ |
| $V_{\omega n}$ Rated wind speed | 12.4 $m/s$ |
| $C_{pMax}$ Maximum power conversion coefficient | 0.411 |
| $\lambda_{Opt}$ Optimal Tip-Speed Ratio | 8.1 |
| $G$ Gearbox ratio | 100 |

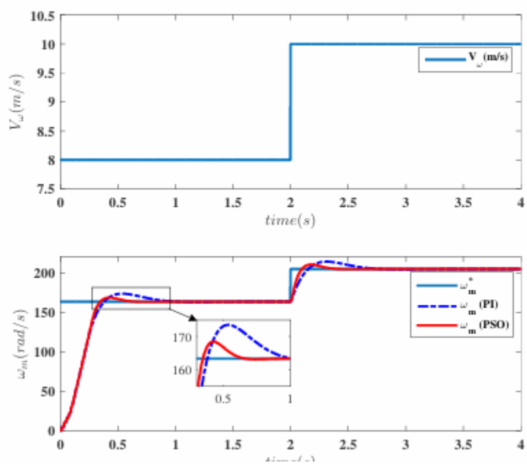


Fig.9. PSO tuned PI controller of the rotational speed with MPPT control.

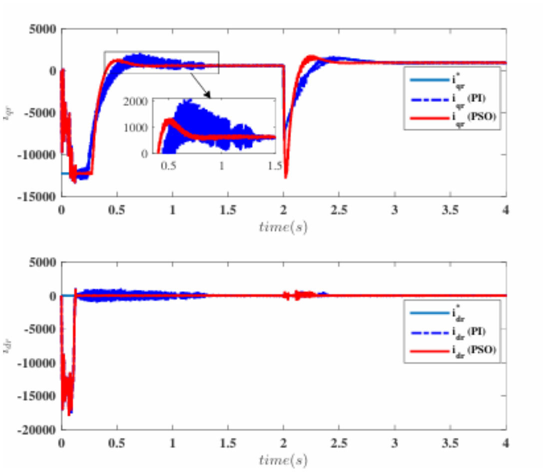


Fig.10. PSO tuned PI controller of the rotor currents with MPPT control.

TABLEIV

MODELVARIABLESDEFINITION.

| Variable | Definition |
|---|---|
| $K_{r1}$ | $\omega_r(L_r\sigma i_{dr} + \frac{L_m v_{qs}}{\omega_s L_s})$ |
| $K_{r2}$ | $\omega_r L_r \sigma i_{qr}$ |
| $K_{g1}$ | $\omega_s L_f i_{dg}$ |
| $K_{g2}$ | $v_{dg} - \omega_s L_f i_{qg}$ |
| $K_{pg} = -K_{qg}$ | $\frac{2}{3} v_{dg}$ |

REFERENCES

[1] M. Cheng and Y. Zhu, “The state of the art of wind energy conversion systems and technologies: A review, ”Energy Conversion and Management,vol.88,pp.332–347,Dec.2014.

[2] H. Ahuja, G. Bhuvaneswari, and R. Balasubramanian, “Performance comparison of DFIG and PMSG based WECS,” in IET Conference on TABLEV PSOALGORITHMPARAMETERS. Parameter Value Coefficientc1 2 Coefficientc2 2 Iterations number Max It 20 Population size Np 10 Renewable Power Generation (RPG2011). Edinburgh, UK:IET,2011, pp.P33–P33.

[3] B.K.Sahu,“Wind energy developments and policies in China: Ashort review,”RenewableandSustainableEnergyReviews,vol.81,pp.1393 1405, Jan.2018.

[4] J.Hu,H.Nian, H.Xu, and Y.He, “Dynamic Modeling and Improved Control of DFIG Under Distorted Grid Voltage Conditions,” IEEE Transactions on Energy Conversion, vol. 26, no. 1, pp. 163–175,Mar. 2011.

[5] M.E.Barrios Aguilar, D.V.Coury, R.Reginatto, and R.M.Monaro, “Multi-objective PSO applied to PI control of DFIG wind turbine under electrical fault conditions,”ElectricPowerSystemsResearch,vol.180, p.106081,Mar.2020.

[6] S.Soued, H.Ramadan, and M.Becherif, “DynamicBehaviorAnalysisforOptimallyTunedOn-GridDFIGSystems,”EnergyProcedia, vol. 162,pp.339–348,Apr.2019.

[7] WeiQiao,WeiZhou, J.Aller, and R.Harley, “Wind Speed Estimation Based Sensorless Output Maximization Control for a Wind Turbine Driving a DFIG,” IEEE Transactions on Power Electronics, vol. 23, no.3,pp.1156–1169,May2008.

[8] L.Huang,B.Yang,X.Zhang,L.Yin,T.Yu, and Z. Fang, “Optimal power tracking of doubly fed induction generator-based wind turbine using swarmmoth–flame optimizer, ”Transactions of the Institute of Measurement and Control,vol.41,no.6,pp.1491–1503,Apr.2019.

[9] E.Rezaei,A.Tabesh,andM.Ebrahimi,“Dynamic ModelandControlofDFIGWindEnergySystems BasedonPowerTransferMatrix,” IEEE Transactions on Power Delivery, vol. 27, no. 3, pp. 1485–1493, Jul. 2012.

[10] A.Tanvir,A.Merabet,andR.Beguenane,“Real-TimeControlofActiveandReactivePowerforDoublyFedInductionGenerator(DFIG)-Based WindEnergyConversionSystem,”Energies,vol. 8,no.9,pp.10389 10408,Sep.2015.

[11] P. Tourou and C. Sourkounis, “Review of control strategies for DFIG-based wind turbines under unsymmetrical grid faults,” in2014 Ninth International Conference on Ecological Vehicles and Renewable Energies(EVER). Monte-Carlo: IEEE, Mar.2014,pp.1–9.

[12] D. Jena and S.Rajendran, “A review of estimation of effective wind speed based control of wind turbines,” Renewable and Sustainable EnergyReviews,vol.43,pp.1046–1062,Mar.2015.

[13] O. Barambones, J. M. Gonzalez de Durana, and E. Kremers, “A neural network based wind speed estimator for a wind turbine control,” in Melecon 2010- 2010 15th IEEE Mediterranean Electro technical Conference. Valletta, Malta: IEEE,2010,pp.1383–1388.

[14] H. Li, K. Shi, and P.McLaren, “Neural-Network-Based Sensor less Maximum Wind Energy Capture With Compensated Power Coefficient,” IEEE Transactions on Industry Applications,vol.41,no.6,pp.1548 1556,Nov.2005.
[15] M.A.Zeddini,R. Pusca,A. Sakly, andM. F.Mimouni, “PSO-based MPPT control of wind-driven Self-Excited Induction Generator for pumping system, ”Renewable Energy,vol.95,pp.162–177,Sep.2016.
[16] K. Ishaque, Z. Salam,M. Amjad, and S.Mekhilef, “An Improved Particle Swarm Optimization(PSO)–Based MPPT for PV With Reduced Steady-State Oscillation,” IEEE Transactions on Power Electronics, vol.27,no.8,pp.3627–3638,Aug.2012.
[17] D.Rekioua,“OptimisationofWindSystemConversion,”inWindPowerElectricSystems. London:SpringerLondon,2014,pp.77–105.
[18] Y.BekakraandD.B.Attous,“Optimaltuning of PI controller using PSO optimization for indirect power control for DFIG based wind turbine with MPPT,” International Journal of System Assurance Engineering and Management,vol.5,no.3,pp.219–229,Sep.2014.
[19] AlhatoandBouall`egue,“Direct Power Control Optimization for Doubly Fed Induction Generator Based Wind Turbine Systems,” Mathematical and Computational Applications, vol.24,no.3,p.77,Aug.2019.